Available online at www.sciencedirect.com

ScienceDirect

Journal of Nutritional Biochemistry 149 (2026) 110193

Journal of Nutritional Biochemistry

ORIGINAL ARTICLE

Dietary galactose enhances systemic lipid oxidation but decreases intestinal fatty acid oxidation in post-weaning female mice

Ferran S. Fos-Codoner, Jaap Keijer, Melissa Bekkenkamp-Grovenstein, Evert M. van Schothorst*

Human and Animal Physiology, Wageningen University, Wageningen, The Netherlands

Received 8 April 2025; received in revised form 4 November 2025; accepted 21 November 2025

Abstract

Replacing part of dietary glucose with galactose in the early post-weaning diet of mice, mimicking extended breastfeeding, improves both short- and long-term physiological and metabolic health parameters. As the primary organ for nutrient absorption, the small intestine was hypothesized to play a key role in these effects.

Young, weaned mice underwent a 3 week dietary intervention comparing isocaloric diets with a monosaccharide fraction of galactose+glucose *versus* glucose. Physiological parameters were assessed in both sexes, while metabolic analyses, transcriptomics, and immunohistochemistry of the proximal small intestine were conducted in fed female mice.

Dietary galactose increased whole-body 24 h fatty acid oxidation (FAO), both absolute and relative to carbohydrate oxidation, without changes in body weight or energy expenditure. Contrasting, the small intestine showed lower expression of transcripts involved in FAO, along with reduced enterocytic lipid droplets. Carbohydrate metabolism remained unaffected, while reduced expression of NADPH-dependent and -independent antioxidant enzymes and the pentose phosphate pathway suggested a shift in local metabolism. Despite these intestinal changes, the liver showed no alterations in lipid catabolism, implicating other organs in the observed systemic FAO increase. In addition, *Ppargc1a*, central regulator of mitochondrial biogenesis was upregulated, which is in line with the known role of galactose in upregulating mitochondrial oxidative phosphorylation.

In conclusion, replacing half of post-weaning dietary glucose with galactose, mimicking prolonged lactose intake, profoundly affects substrate metabolism at both systemic and intestinal levels. We propose that reduced intestinal FAO redirects fatty acid oxidation to extra-intestinal, extra-hepatic tissues, driving the observed systemic metabolic benefits.

Keywords: Gut; metabolism; enterocyte; fatty acid oxidation; RER; NADPH; oxidative stress.

1. Introduction

During the lactation period, breast milk stands as the primary source of nutrition for offspring, offering essential nutrients crucial for their growth and development. As this phase transitions into weaning, solid foods are gradually introduced into the infant's diet, marking a pivotal shift in nutritional intake [1,2]. The carbohydrate fraction of the diet undergoes a substantial change around weaning, with the predominantly glucose- and fructose-based weaning foods contrasting with the predominantly lactose-based composition of breast milk and infant formula. Lactose, a disaccharide comprised of glucose and galactose, constitutes the primary carbohydrate source in early nutrition and represents approximately 40% energy of milk [3].

Upon consumption, lactose is enzymatically hydrolysed into glucose and galactose by β-galactosidase on the brush border of the intestinal enterocytes [4]. Although galactose shares the chemical composition of glucose, its oxidation rate for cellular energy production is different [5]. This can be attributed to the few additional steps that galactose must undergo to be fully oxidized, the Leloir pathway where galactose is converted into the glycolytic intermediate glucose-6-phosphate [6]. Additionally, galactose can be metabolized through alternative pathways, such as the formation of galactitol or galactonate [7]. The metabolic significance of these alternative pathways, especially in young individuals, is not well understood.

The differences between oxidation of galactose and of glucose result in marked physiological effects, especially when it comes to energy metabolism. In cell culture models, galactose induces a

* Corresponding author at: Human and Animal Physiology, Wageningen University, Postbus/PO Box 338, 6700AH, Wageningen, The Netherlands.
E-mail address: evert.vanschothorst@wur.nl (E.M. van Schothorst).

https://doi.org/10.1016/j.jnutbio.2025.110193

switch from glycolysis towards mitochondrial oxidative phosphorylation (OXPHOS) [8]. Such a switch was also validated *in vivo* in intestinal mucosa of young post-weaning female mice in the post absorptive state [9].

The composition of diets, particularly their carbohydrate content and composition, influences the utilization of various substrates. At the whole-body level, this is reflected in variations in the respiratory exchange ratio (RER) [10]. Additionally, the utilization differences of substrates likely lead to varying contributions of specific organs to the overall RER. Previously, we observed a marked effect of post-weaning galactose consumption on intestinal mucosal metabolism. In a post absorptive state, where mice were food deprived for 2 to 5 h, we observed a marked increase of mitochondrial oxidative metabolism, accompanied by an upregulation of both glucose and fructose oxidation pathways compared to the control diet that lacked galactose [9]. Here, we aimed to further understand how galactose affects intestinal energy metabolism. For this, we executed a comparable dietary intervention study but focused specifically on the fed state. We investigated body, metabolic, molecular and immunohistochemical parameters, including the proximal small intestine and the liver.

2. Materials and methods

2.1. Animals and experimental setup

All experimental procedures involving animals received approval from both national and local Animal Experimental Committees (AVD1040020171668) and adhered to the guidelines outlined in the EU directive 2,010/63/EU. The mice were kept in Makrolon type II cages with bedding, cage enrichment and nesting material, at a constant temperature of 23°C±1°C, humidity at 55±15%, under a 12:12 light-dark cycle. The mice had unrestricted access to water and a standard rodent chow diet (AM-II, AB Diets, Woerden, The Netherlands). Breeding pairs (C57BL/6JRccHsd mice) were obtained from Envigo (Horst, The Netherlands) and were time-mated while on the standard diet. Litters were standardized to six pups per nest (three males and three females) on postnatal day (PN) one or two, and redistributed over cross-fostering dams. This day was considered day PN1.

On PN21, pups were weighed and had their body composition (fat mass (FM) and lean mass (LM)) determined using an EchoMRI 100 V (Echo Medical Systems, Houston, TX, USA). Following this, pups were stratified by body weight (BW), housed individually, and assigned to one of two diets for 3 weeks: a diet containing 32 energy% (en%) glucose (Glu group, n=13) or a diet containing 16 en% glucose and 16 en% galactose (Gal group, n=13) representing a lactose mimic, while all other dietary components were kept equal, including 32 en% starches, 3 en% fructose and 20 en% fat, based on the BIOCLAIMS diet [11] (Supplemental Table 1). Diets were provided by Ssniff (Soest, Germany) and detailed dietary compositions are provided in Supplemental Table 1. BW, FM, LM, water intake, and food intake were monitored weekly. Specific metabolic measurements were performed between PN35-PN42 (see below).

On PN42, after measurement of BW, FM, and LM, the animals were euthanized by decapitation between two to 5 h after the start of the light phase. The small intestines were cut into two equal-length parts measured from the pylorus to the ileal-caecal valve (called proximal and distal parts). Of the proximal part and the proximal side, the first centimeter was discarded, and the next cm was isolated and fixed for 24 h in 4% paraformaldehyde (PFA) and embedded in paraffin for histological analysis; of the distal side the last cm was isolated, fixed and embedded in paraffin. The remaining central parts were opened, rinsed in ice-cold PBS, and the mucosa was scraped, collected, and snap frozen. Livers were collected, lobes separated, snap frozen in liquid nitrogen, and stored at −80°C for further analysis; the right lobe was used for molecular measurements. BW, FM, LM, food intake (FI) and water intake (WI) were measured in both sexes. Indirect calorimetry and molecular analysis were performed only in females since previous studies showed larger effects of dietary galactose in female mice [12].

2.2. Indirect calorimetry

Indirect calorimetry (InCa) was performed from PN35 to PN38, using a Phenomaster LabMaster Metabolism Research Platform (TSE Systems GmbH, Bad Homburg, Germany) as published [13], with the following configurational updates: 12 cages were upgraded to 24 cages together with higher resolution physical activity frames (ActiMot 3) with beams at a distance of 5 mm each instead of 15 mm, and sensors for food and drink intake. All gas sensor units were duplicated to keep the same sample interval. Continuous measurements of oxygen consumption, total carbon dioxide production (sum of $^{12}CO_2$ and $^{13}CO_2$ measurements), methane (CH_4), voluntarily locomotor activity, water intake, and FI were conducted, with subsequent calculations of RER and energy expenditure (EE), as published [13].

The system has dual air drying units and is employed with dual ABB (ABB Automation, Frankfurt am Main, Germany) units for gas analysis, utilizing internal calibration cells for $^{12}CO_2$, $^{13}CO_2$, and CH_4, based on [14]. A single reference cage was used across both dual systems. Measurements were recorded at intervals of 1′32″ per cage, resulting in three data points per hour for each cage. Before each run of measurements, gas sensor units were calibrated using specific calibration gasses (Linde Gas Benelux BV, Dieren, The Netherlands): zero (20.947% O_2 in N_2), and span (0.5% O_2 in N_2) gasses.

The first day of measurements served as an acclimation period. The data from the subsequent 24 h (covering one 12 h light phase (LP) and one 12 h dark phase (DP)) were used for analysis. ANCOVA analysis of EE using LM as a covariant showed no statistical difference (P=.75), *i.e.*, only mass-dependent effects between groups [15] and we therefore report raw EE values.

Relative carbohydrate and lipid oxidation levels were calculated using equations 4 and 5 from [16], resp. with its basis being the RER conversion table by Péronnet & Massicotte [17]. This novel method allows us to accurately convert the experimentally obtained RER values (VCO2/VO2) into percentages of carbohydrate and lipid oxidation. Next, using equations 1 and 2 from [14], the relative glucose and lipid oxidation levels were combined with the EE obtained from our InCa system for the same animal at each and every datapoint, which provides absolute levels of total (mg per minute) carbohydrate oxidation and total lipid oxidation.

2.3. RNA isolation and RNA sequencing

Total RNA was isolated from the intestinal scrapings and the liver's right lobe using the RNeasy mini kit (Qiagen, Hilden, Germany). Integrity of RNA was checked with Agilent 2,100 Tape Station (Agilent Technologies, Santa Clara, CA). All samples passed the integrity quality standards. Strand-specific transcriptome resequencing was performed on total RNA isolated from proximal intestine scrapings. RNA preparation, library construction and sequencing using DNBSEQ technology were performed at Beijing Genomics Institute (Shenzhen, Guangdong, China). Clean and filtered reads were obtained in FASTQ format, and quality check was performed using FASTQC [18]. Reads were aligned to the mouse genome (GRCm39.108) using STAR [19] and counts were quantified using HTSeq [20]. Average sequencing depth was 24.1 M paired end reads, of which at least 92% were uniquely mapped.

2.4. RNASeq Transcriptome analysis

Data and statistical analyses were performed in R version 4.3.1. DESeq2 version 1.42.0 [21] was used to identify differentially expressed genes (DEGs) between the Gal (n=13) and control Glu (n=13) groups. An extra filtering step with the removal of genes with less than a total of 10 reads per row was applied. Benjamini–Hochberg multiple testing correction was used to obtain adjusted P-values (p.adj) at a false discovery rate (FDR) of 5%. Heatmaps were made using rlog transformed data, with library size correction. All data has been deposited in Gene Expression Omnibus (GEO) with ID GSE255078. Gene Ontology (GO) enrichment analysis (enrichGO) for biological processes was performed in R using ClusterProfiler [22]. Only significant transcripts were used for the analysis with an adjusted P-value <.05.

2.5. Quantitative RT-PCR

Liver gene expression analysis was performed by RT-qPCR using iQ SYBR Green Supermix (Bio-Rad Laboratories Veenendaal, The Netherlands) on a CFX96 Touch Real-Time PCR Detection System (Bio-Rad). cDNA was synthesized using the iScript kit (Bio-Rad). Primers were designed using NCBI Primer-BLAST, with details of primer sequences and annealing temperatures provided in Supplemental Table 2. Pooled cDNA from all samples underwent serial dilutions to create standard curves, and two negative controls (water and a sample without reverse transcriptase) were included for each transcript. cDNA samples were analysed at a 100-fold dilution, with both samples and standards measured in duplicate. The RT-qPCR protocol included 3 min at 95°C, followed by 40 cycles of 15 s at 95°C and 45 s at the specified annealing and elongation temperature, ending with a melt-curve analysis. Stable gene expression was determined using Bio-Rad CFX Maestro software (version 4.1; Bio-Rad), and the data were normalized to reference genes Calnexin (*Canx*), Beta-2 microglobulin (*B2m*) and ribosomal protein S15 (*Rps15*). The control Glu group was set to unity to display normalized gene expression.

2.6. Histology

The proximal small intestine fixed in 4% PFA for 24 h at 4°C was embedded in paraffin blocks and cut into 5 μm thick sections. Sections were dewaxed in xylene and rehydrated for staining. An epitope-specific antibody was used for the detection and quantification of the lipid droplet marker Perilipin 2 (PLIN2) (1:200; 15,294-1-AP ThermoFisher, Schwerte, Germany). After rehydration, sections were washed with tris buffered saline (TBS; TRIS-HCl pH 7.6- with 10 mM NaCl) and the antigen was retrieved using 10 mM sodium citrate pH 6.0 for 10 min at sub-boiling temperatures in the microwave. Sections were left to cool for 30 min at room temperature (RT) and washed 5 times for 5 min each with TBS. Tissue sections were blocked with 5% goat serum (S-1,000, Vector Laboratories, Newark, CA) for 30 min at RT. The sections were then incubated with the primary antibody against PLIN2 (1:200 in TBS with acetylated bovine serum albumin (BSAc) 1:2,000) overnight at 4°C. After 3 washes in TBS the sections were then incubated with the secondary antibody Alexa 594 goat antirabbit (1:200 in TBS-BSAc; A11012; Invitrogen, Carlsbad, CA) for 1 h at RT. The nuclei were stained with 4′,6-diamidino-2-phenylindole (DAPI; 1:10,000 in TBS-BSAc; D9564; Sigma-Aldrich, Saint Louis, MO) for 5 min at RT; Rabbit IgG (Vector Laboratories) control was used to correct for nonspecific binding. Sections were mounted with Fluoromount-G (0100-01; Southern Biotech, Birmingham, AL) and dried in the dark at 4°C overnight.

Table 1
Visual quantification of lipid droplets in liver sections.

Visual quantification grade	Number of lipid droplets
0	No lipid droplets are observed
1	Few lipid droplets are observed
2	Medium number of lipid droplets are observed
3	High number of lipid droplets are observed
4	Very high number of lipid droplets are observed

2.7. Image acquisition processing and quantification

The images were taken with a Leica DM6b microscope (Leica Micro Systems Inc.). Quantification was performed by visual examination of the whole section under the fluorescence microscope. For each mouse (Glu n=6, Gal n=7) 1 to 3 technical replicates were analyzed. In a blinded manner, two researchers independently scored the staining according to Table 1. Technical replicate scores did not differ in score from each other and the score from the two researchers was averaged. Representative images for each score can be found in Supplemental Fig. 1.

2.9. Serum and liver triglyceride measurement

Serum and liver obtained during sacrifice was used to measure circulating and tissue triglycerides (TG) levels (Liquicolour kit, Human). Liver TG levels were normalized using sample weight.

2.8. Statistics

DEG and pathway analysis were done using R version 4.3.1. RER, EE, BW, FM, LM, food and water consumption and activity were analysed using Student's t-test based on normal distributed data. Statistical analysis of the histological scores was performed using Student's t-test for nonparametric samples (Mann–Whitney U test) between the two dietary groups. All the aforementioned tests were performed using Graphpad Prism 9.3.1 (Graphpad Software, San Diego, CA). P<.05 was considered significant and indicated as follows: $^{*}P$<.05, $^{**}P$<.01, $^{***}P$<.001. Details on statistics regarding the omics data can be found under *2.4 RNASeq Transcriptome analysis.*

3. Results

3.1. Post-weaning galactose consumption does not affect body weight and body composition of mice

Following the 3 weeks isocaloric dietary intervention period, the effects of galactose (Gal: diet containing both galactose and glucose each at 16 en% as monosaccharide fraction) *versus* glucose (Glu: 32 en% as monosaccharide fraction in an otherwise identical diet, also containing starch (Supplemental Table 1) were compared. In the female mice, no differences were seen in the mean body weight and body composition (lean and fat mass) between both groups (Fig. 1A–C). In contrast, a significant increase in food and water consumption was observed for the female Gal mice, which is in line with previous results in female mice [13]. Male mice showed similar patterns comparable to the female mice for BW, body composition, and food and water intake (Supplemental Fig. 2). Further analyses were done using female mice because of the more prominent galactose-induced programming effects previously observed [12].

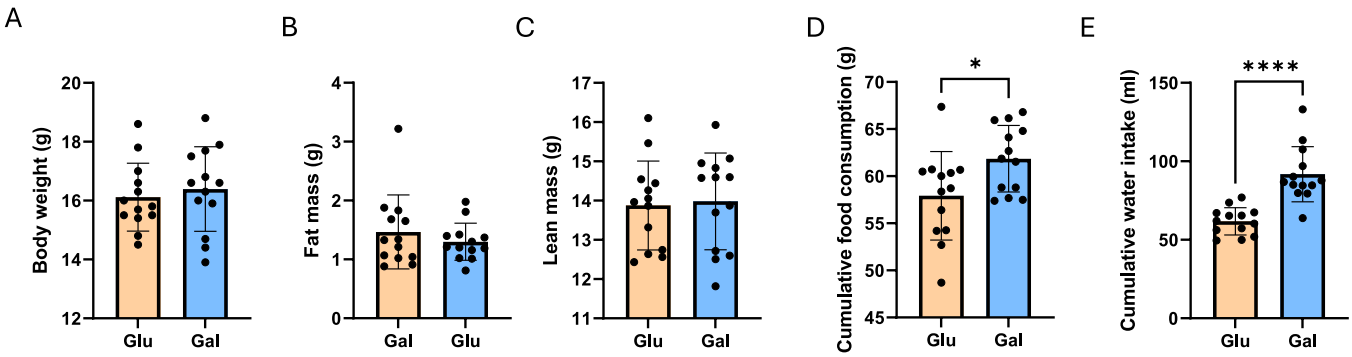

Fig. 1. Body weight, body composition, and cumulative food and water intake in females fed control Glu diet (orange bars) or Gal diet (blue bars). (A) Body weight and (B, C) body composition at PN42, and 3 weeks (D) cumulative food and (E) water intake. Despite similar mean body weight and composition, mean cumulative food and water intake over the 3 weeks intervention period (PN21-PN42) was higher in the Gal *versus* Glu fed mice (D, E). Differences between groups were analyzed using Student's t-test. Values are expressed as mean±SD (n=13).

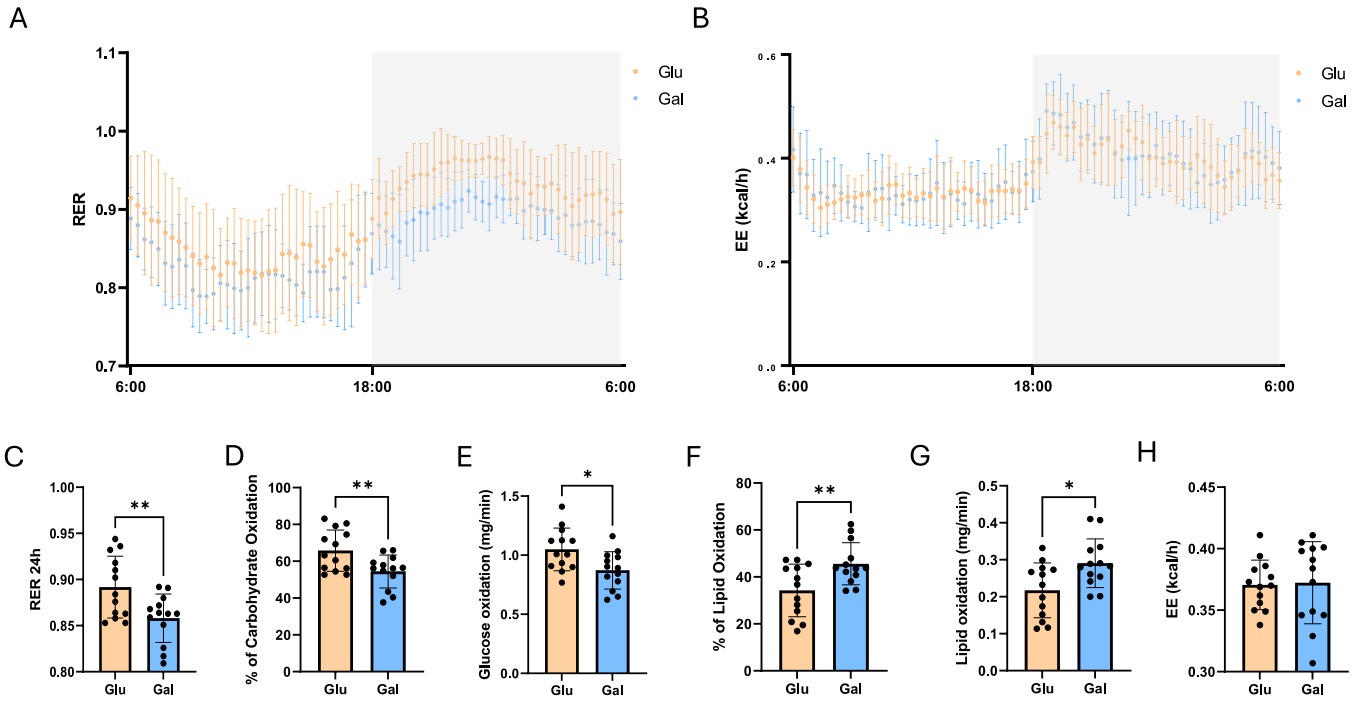

Fig. 2. Twenty four hours energy metabolism. (A) respiratory exchange ratio (RER), (B) energy expenditure (EE), (C) mean RER over 24 hr, (D) % carbohydrate oxidation and (E) total carbohydrate utilization, (F) % lipid oxidation, (G) total lipid oxidation, and (H) mean EE over 24 hr. Differences between groups were analyzed using Student's t-test. Values are expressed as mean±SD (n=13).

3.2. Post-weaning galactose consumption significantly shifts whole body substrate utilization without changes in energy expenditure

Substrate utilization and whole-body metabolism were investigated by indirect calorimetry (InCa) in female mice. The Gal fed females showed a significant lower RER, which reflects a higher % lipid oxidation and lower % carbohydrate oxidation. (Fig. 2A, C, D, and F; Table 2). This decrease in mean RER was observed for the full 24 h, as well as for the active dark phase, but not for the inactive light phase (Table 1). However, no significant differences in energy expenditure (EE) and activity during the 24 h period were observed (Fig. 2B and H; Table 1). In addition, taking RER and EE into account, in the Gal group total 24 h carbohydrate and lipid oxidation were also significantly reduced and increased, respectively (Fig. 2E and G). During the 24 h InCa recording, food intake was similar between the groups (Glu: 5.36 g±0.98; Gal: 5.21 g±1.25; P=.7). Again, 24hr water intake was significantly higher in the Gal animals (Glu: 5.05 ml ±1.09; Gal: 7.64 ml ±2.23; P=.001), consistent with the 3-weeks cumulative water intake (Fig. 1E).

3.3. Post-weaning galactose consumption downregulates proximal small intestinal fatty acid metabolism in fed mice

The small intestine is responsible for the absorption of most dietary components, including galactose and glucose. Given that after ingestion monosaccharides are largely absorbed in the first part of the small intestines (duodenum and jejunum), our study primarily focused on the molecular effects within the proximal small intestine of the female mice in the fed state. Notably, an abundant amount of chyme, partially digested food from the stomach, was observed throughout the entire length of the small intestine, confirming that the mice were sacrificed in the fed state. Mucosal scrapings from the proximal small intestine were used for RNASeq analysis. Out of over 20,000 transcripts, 801 (adjusted P-

Table 2
Whole body indirect calorimetry results for energy expenditure (EE), respiratory exchange ratio (RER), and activity (average beam breaks).

Parameter		Glu	Gal	*P*-Value
EE	LP	0.33±0.02	0.33±0.03	.99
	DP	0.41±0.02	0.41±0.03	.79
RER	LP	0.85±0.05	0.82±0.03	.10
	DP	0.93±0.03	0.89±0.03	.002**
Activity	24h	4,945±1,737	6,290±1,838	.06
	LP	2,234±1,059	3,174±1,482	.07
	DP	7,657±2,750	9,406±2,836	.12

Values are expressed as mean±SD (n=13).
Abbreviations: DP, dark phase; LP, light phase.
** $p < 0.01$.

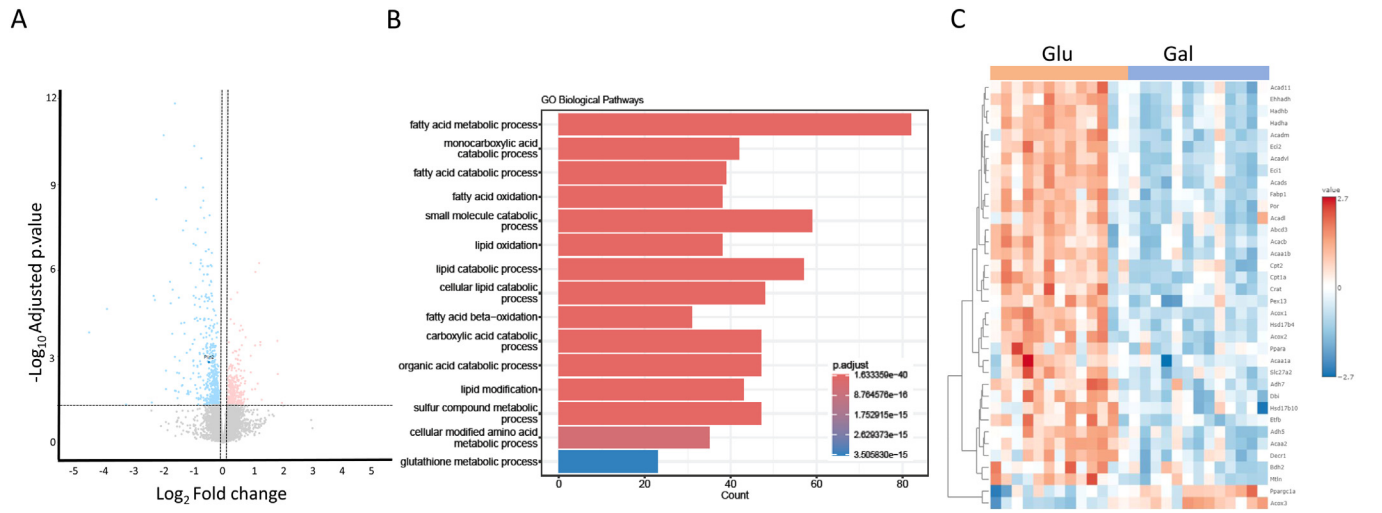

Fig. 3. Overview of the transcriptional effects of post-weaning galactose consumption in proximal small intestinal mucosa. (A) Volcano plot of significance and Log_2 fold change (FC) of all transcripts in Gal *versus* Glu. Dotted lines indicate absolute log_2FC=0.1 and *P*.adjusted with a FDR=0.05. Higher expressed transcripts are shown in red, those being lower expressed in blue. (B) Top 15 most regulated pathways based on gene ontology (GO) enrichment analysis. (C) Heatmap of all significant transcripts with the GO term 'fatty acid oxidation'.

values (p.adj) <.05) were significantly affected in the Gal *versus* Glu group with more lower expressed transcripts than higher expressed ones in Gal (Fig. 3A). RNASeq data was validated by RT-QPCR for two transcripts (Supplemental Fig. 3). Pathway analysis using gene ontology (GO) enrichment showed that of the top 15 most significantly different pathways, 12 were related to fatty acid metabolism, in particular FAO (Fig. 3B). The remaining three relate to redox homeostasis and modified amino acid metabolism. To confirm the directionality and consistency of the observed effects in FAO, all 36 significant transcripts with the GO term "fatty acid oxidation" were selected and plotted as heatmap (Fig. 3C).

All but two showed a significant lower expression in the Gal group, highly supporting the downregulation of FAO in the proximal small intestines (Fig. 3C). Acyl-Coenzyme A oxidase 3 (*Acox3*) and peroxisome proliferative activated receptor, gamma, coactivator 1 alpha (*Ppargc1a*), the latter encoding the master regulator of mitochondrial biogenesis PPARGC1A [23], were higher expressed.

Among the intestinal FAO genes that exhibited downregulation following the galactose intervention was the transcription factor *Ppara*. Given the central role of PPARA in regulating fatty acid metabolism, the expression of its FAO target genes was further analysed. Notably, all PPARA target genes involved in FAO [24] that showed a significant regulation displayed lower expression levels in the galactose group compared to the glucose control group, ranging from mitochondrial uptake of fatty acids to their full oxidation, and peroxisomal FAO (Fig. 4). Other PPARA

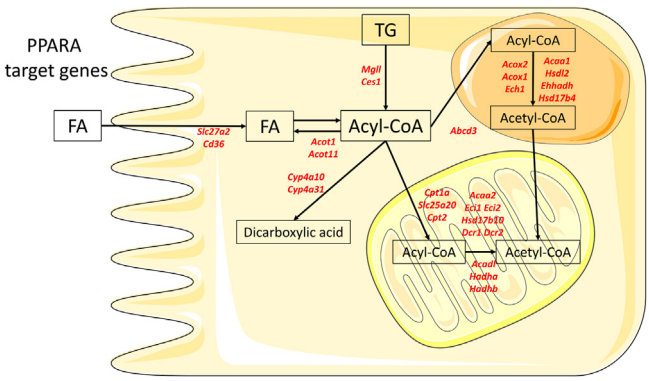

Fig. 4. Schematic representation of PPARα's targets involved in FA metabolism in proximal small intestinal enterocytes. All the displayed transcripts (red) were significantly lower expressed in the galactose group, and no PPARα targets were upregulated. Orange organelle: peroxisome; yellow organelle: mitochondrion.

targets involved in microsomal (ω-hydroxylation) or ketone body metabolism also showed a consistent significant lower expression in the Gal fed mice. Simultaneously, no differential effects were observed in inflammation-related targets of PPARA. Overall, 45 out of the 147 described PPARα target genes involved in lipid metabolism [25] were significantly regulated by galactose.

Besides FAO for energy supply, proximal enterocytic fatty acid metabolism can be divided into fatty acid uptake (from intestinal lumen), storage (as TG), and the inclusion of FA into chylomicrons being subsequently secreted into lymph for transport to other organs. Uptake of lipids from the lumen appeared to be lower, based on transcript levels of fatty acid transporters *Cd36* and *Slc27a2*. Epithelial storage and secretion were subsequently investigated in more detail. In addition, *de novo lipogenesis* seems to be only mildly affected, without changes in key transcripts like Acetyl-CoA carboxylase alpha (*Acaca*) and Fatty acid synthase (*Fasn*), but with an increased expression of ATP-citrate lyase (*Acly*) in the Gal group (Supplemental Fig. 4).

3.4. Lipid droplet associated transcripts show a lower expression upon galactose consumption

Epithelial storage of fatty acids involves triglyceride (TG) synthesis and subsequent trapping in lipid droplets. Transcripts encoding enzymes synthesizing TG from FAs and glycerol-3-phosphate all appeared not to be different. The main marker for lipid droplets is perilipin 2 (PLIN2). Its transcript appeared significantly lower expressed in the small intestine (Fig. 5A). A lower lipid droplet accumulation in the small intestinal mucosa was supported by the significant regulation of 33 lipid droplet related transcripts (31 lower expressed, 2 higher expressed) (Fig. 5B), out of the reported 171 [26]. The high percentage of lower expressed lipid droplet-associated transcripts strongly suggests a reduction in the lipid droplet content in the small intestinal mucosa.

To further confirm this, PLIN2 immunostaining was performed on a section of the proximal small intestine. Indeed, a lower presence of lipid droplets was observed in those mice that received galactose during the post-weaning time (Fig. 5C and D), with a detailed picture of the LD morphology shown in Fig. 5E.

3.5. Secretion of TG as chylomicrons into circulation

The final step in the fatty acid-linked pathways within enterocytes involves their secretion into the circulation via chylomicrons. This process is associated with the activity of genes encoding the apolipoprotein family. None of the chylomicron-associated apolipoproteins [27] appeared to be regulated. Only the apolipoprotein L subgroup (specifically transcripts *Apol10a* and *Apol10b*), encoding proteins associated with high-density lipoprotein (HDL) particles, showed significant regulation, with higher expression levels in the galactose-fed mice.

Overall, this suggests that in the proximal small intestinal mucosa, the uptake of fatty acids and their subsequent oxidation (FAO) is lower expressed, while the transcriptional regulation of fatty acid export is hardly affected. Simultaneously, storage of TG is lower in this tissue in the Gal mice. Nevertheless, the levels of circulating TG did not differ significantly between the two dietary groups (Glu: 59.36±15.48 mg/dl; Gal: 64.85±17.98 mg/dl; P=.4).

3.6. NADPH, redox, and PPP transcripts are downregulated by post-weaning galactose consumption

In the GO pathway analysis glutathione metabolism and glutathione related pathways ("Sulfur compound metabolic process" and "Cellular modified amino acid metabolic process") also emerged within the top 15 regulated pathways (Fig. 3B). Zooming in on individual genes involved in NADPH-dependent antioxidant defense, glutathione reductase, glutathione synthetase, thioredoxin reductase and peroxiredoxins were all downregulated. In addition, transcripts for NADPH-dependent detoxifying proteins were also downregulated (Fig. 6A). Furthermore, most transcripts encoding cytoplasmic NADPH-producing enzymes (glucose-6-phosphate dehydrogenase (*G6pdx),* phosphogluconate dehydrogenase (*Pgd*), malic enzyme 1 (*Me1),* and isocitrate dehydrogenase 1 (*Idh1*)), including those within the pentose phosphate pathway (PPP) (Fig. 6B), were also downregulated. The antioxidant enzymes *Sod1* and *Catalase,* which are not directly dependent on NADPH, also showed a lower expression. The aforementioned NADPH-producing enzymes were all highly correlated with all the antioxidant genes that are shown in Fig. 6A (Supplemental Table 3). The consistent lower expression of antioxidant and NADPH generating enzymes in association with lower expression of FAO-transcripts suggests that NADPH production is reduced in response to reduced oxidative stress, requiring less antioxidant defense. We could see this by the also significant correlations between the transcripts of the aforementioned NADPH-producing enzymes with the FAO transcripts depicted in Fig. 3C (Supplemental Table 4).

3.7. Alternative pathways of galactose metabolism in small intestine

In contrast to lipid and redox metabolism, carbohydrate metabolism only showed minor differences between the Gal *versus* Glu groups, even though we studied a monosaccharide intervention. Nevertheless, a close examination of the Leloir pathway enzymes in the small intestinal mucosa revealed an unexpected marked and significantly reduced expression in the galactose fed mice of Galactokinase (*Galk1*), the first step of this pathway. Besides the Leloir pathway that cells use to metabolize galactose, two alternative galactose metabolizing pathways have been described. The first one is the conversion of galactose into galactitol via aldose reductase (*Akr1b3*), which was significantly lower expressed ($Log_2FC=-0.36$, $P<.001$). Regretfully, we did not collect urine in this study, because we assumed it would tell little about the intestine functionality. We therefore resorted to urine samples obtained from 3 to 5 h food-deprived female mice from a previous study, exposed to the same dietary intervention for the same duration [13]. Urine analysis showed that galactitol levels were significantly higher in the Gal group *versus* Glu group (Gal: 8.9±1.9 mg/ml, Glu: 3.3±1.8 mg/ml, P=.02). The second alternative pathway is via galactose dehydrogenase and the subsequent formation of galactonate. Regretfully, no genes encoding for this step have been annotated. However, since this pathway is described at the metabolite level [28], we resorted to analysis of the end-product. We measured tissue galactonate levels by standard high pressure anion exchange chromatography (HPAEC). However, intracellular concentrations of galactonate in small intestinal mucosa were undetectable, therefore the contribution of this pathway seems minor, at least under our experimental conditions

3.8. Post-weaning galactose consumption does not affect hepatic fatty acid metabolism gene expression

The transcriptome analysis of the small intestines revealed a lower expression of FAO transcripts, while higher relative and absolute whole-body FAO levels were seen. Therefore, we next assessed the liver's contribution by targeted qPCR analysis of FAO transcripts. This showed no significant differences between the two dietary intervention groups. Hepatic fatty acid binding protein 2 (*Fabp2,* intracellular FA transporter), acyl-Coenzyme A oxidase 1 (*Acox1*, peroxisomal FAO), carnitine palmitoyltransferase 1a (*Cpt1a*, rate-limiting mitochondrial FA importer), hydroxyacyl-CoA dehydrogenase (*Hadha*, mitochondrial FAO), and acetyl-Coenzyme A acetyltransferase 2 (*Acat2*, cholesterol synthesis) were all not changed (Fig. 7A–E). In addition, total hepatic TG levels were not

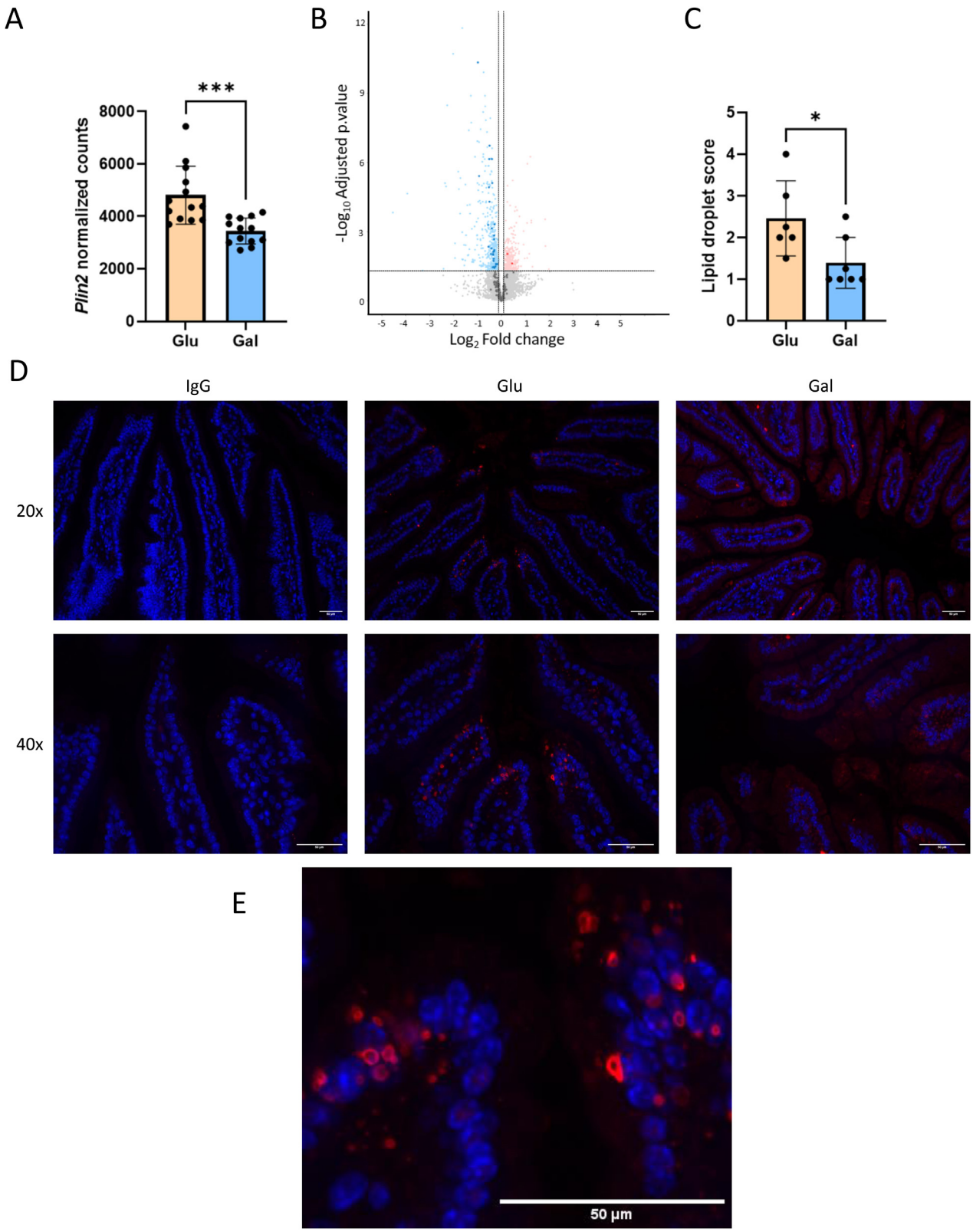

Fig. 5. Small intestinal lipid droplets (LD) and the transcripts of lipid droplets-associated proteins are reduced in the galactose intervention group. (A) Normalized expression counts of *Plin2*, encoding the main LD-associated protein in enterocytes. Differences between groups were analyzed using Student's t-test. (B) Representation of the regulated transcripts of LD-associated proteins. The 171 LD associated transcripts are shown in bold. Grey: not regulated, blue: lower expression, red: higher expression. (C) Quantification of the number of LDs based on LD score of the small intestinal sections stained for PLIN2, Differences between groups were analyzed using Mann-Whitney U test for non-parametric samples. (D) Representative pictures of negative control (IgG), glucose-fed mice group (Glu) and galactose-fed mice (Gal) at 20x and 40x magnification. (E) Zoomed-in picture of the PLIN2 staining depicting the morphology and size of the lipid droplets. Blue: nuclear DAPI stain, red: PLIN2-specific stain. Scale bar 50µ m.

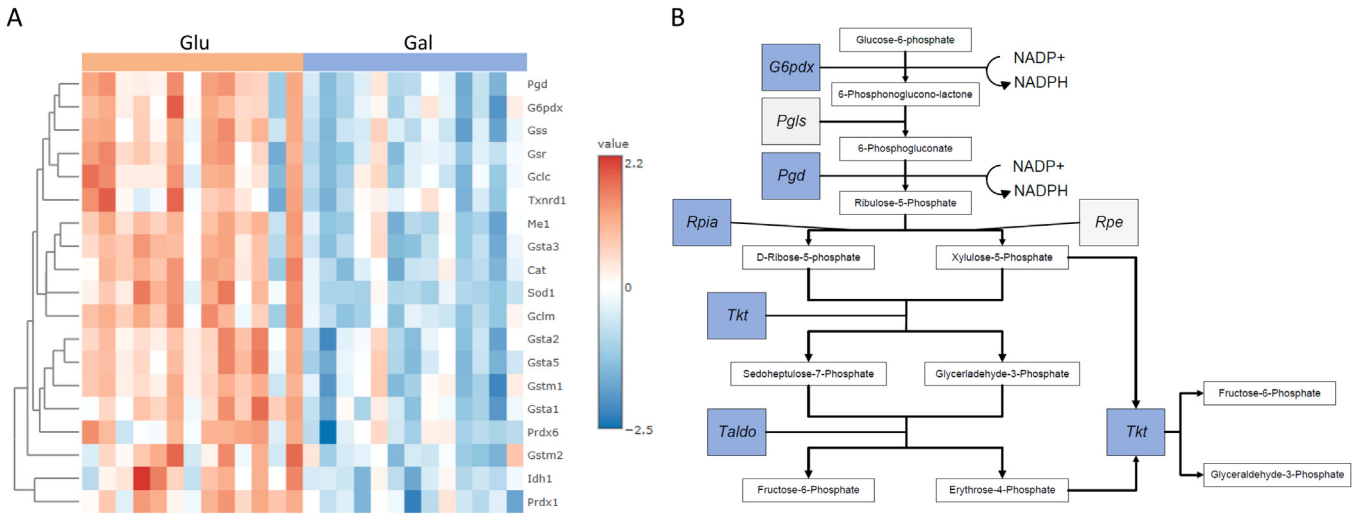

Fig. 6. Overview of the transcriptional effects of dietary galactose in NADPH and redox related transcripts and the pentose phosphate pathway (PPP). (A) Heatmap showing expression of all significant redox related transcripts. (B) Galactose intervention effects on the PPP. Transcripts are boxed. Blue: downregulated, red: upregulated (absent), grey: not regulated, based on p.adj < 0.05 in the RNAseq dataset.

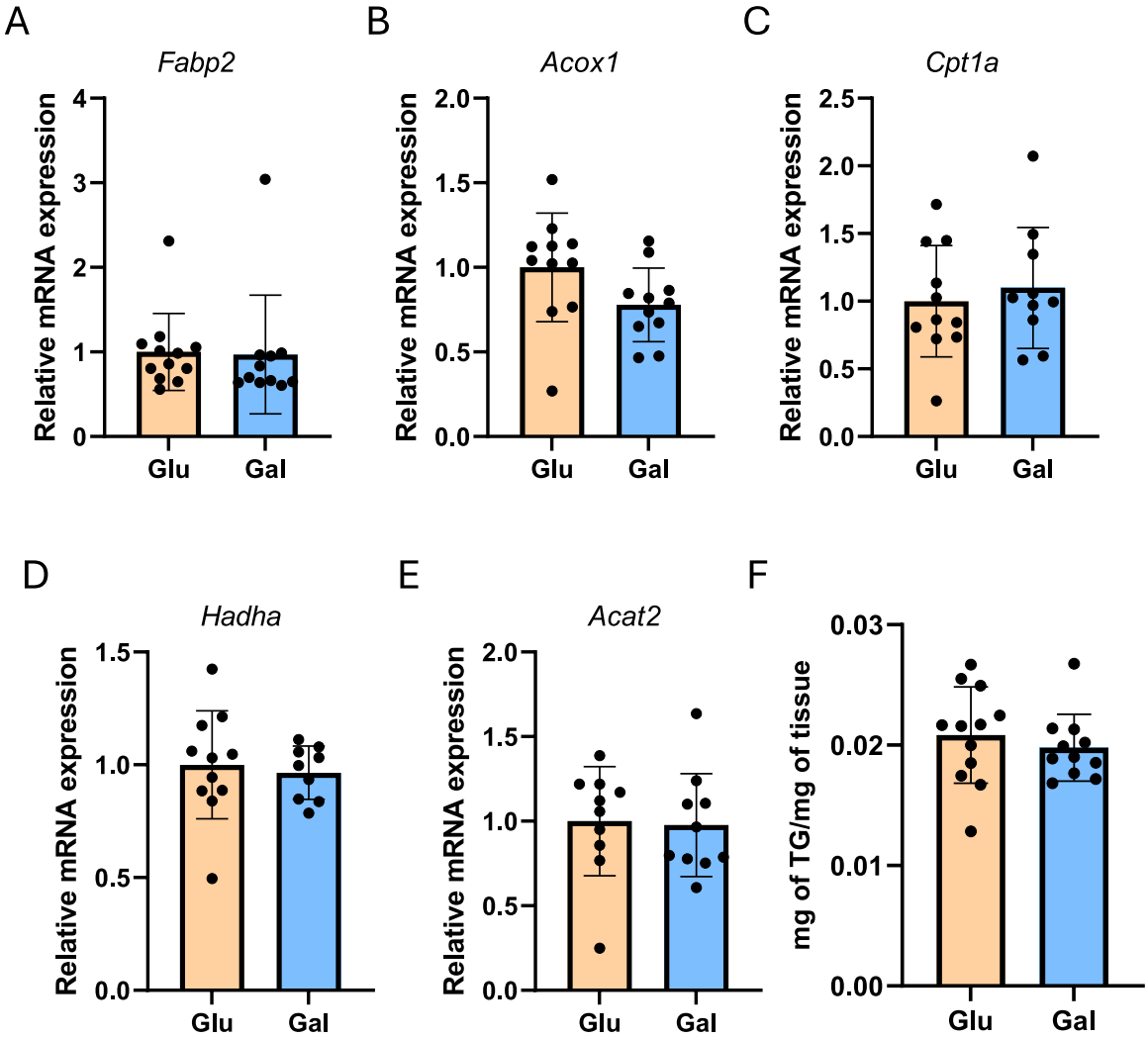

Fig. 7. Expression of selected hepatic transcripts involved in fatty acid metabolism in liver. (A) Fabp2, (B) Acox1, (C) Cpt1a, (D) Hadha, and (E) Acat2. (F) Total hepatic triglyceride levels. Expression is presented as arbitrary units relative to the expression of the reference genes Canx, B2m, and Rps15. Differences between groups were analyzed using Student's t-test.

different between the groups (Fig. 7F). This suggests that the galactose intervention did not significantly impact hepatic fatty acid metabolism.

4. Discussion

To further understand the beneficial metabolic health effects of galactose intake previously observed in fasted in young mice [9,13], we here studied the fed situation. We further focused on the small intestine since it is crucial for nutrient digestion and absorption, sensing, and signaling, serving a dual role as a gatekeeper and metabolic organ. We examined whole-body substrate utilization and small intestine gene expression effects of galactose consumption during the 3 weeks following lactation. Replacing part of the dietary glucose with galactose during this period significantly impacted energy metabolism at both the whole-body and the small intestinal level. Our findings in fed female mice newly indicated that galactose consumption triggered a shift towards a higher whole-body relative and absolute fat oxidation, without affecting body weight, whole-body lean and fat mass, or energy expenditure. In apparent contrast, in the proximal small intestinal mucosa we observed a markedly lower expression of FAO transcripts and lower TG storage based on perilipin 2 staining, the main marker of intracellular lipid droplets. The observed metabolic effects were assessed in females; however, males included in the study exhibited similar body weight and body composition growth curves, suggesting that the effects are highly comparable in males.

Due to its unique metabolic properties, galactose can significantly impact energy metabolism, particularly mitochondrial metabolism. In this study, we observed a significant increase in the expression of *Ppargc1a*, the master regulator of mitochondrial biogenesis [23] in the galactose group (Fig. 3C). This finding is consistent with previous *in vivo* studies, which demonstrated an increase in OXPHOS, where the expression of all significantly regulated OXPHOS transcripts from all complexes was higher upon galactose consumption [9]. Additionally, in vitro studies using intestinal cell cultures have shown that galactose increases mitochondrial oxidative phosphorylation (OXPHOS) [8]. The greater reliance on mitochondrial OXPHOS is likely due to the lower efficiency (rate per time unit) of galactose oxidation compared to glucose in ATP production. The lower efficiency of galactose metabolism compared to glucose may contribute to the increased whole-body fat oxidation (FAO) observed in the Gal animals. This aligns with previous findings of greater whole-body lipid utilization after galactose consumption compared to glucose in obese women [29]. Although this agrees with a shift from glycolysis to mitochondrial oxidative metabolism, it is somewhat surprising in view of abundant availability of glucose in the fed state of the animals. Of note, the higher whole body lipid oxidation was especially seen in the dark phase, when the animals consume most of their food (LP: 0.61 $g\pm0.29$; DP: 1.97 $g\pm0.8$; $P<.0001$).

Possibly a decreased insulin response upon galactose compared to glucose intake may contribute to this observation or may be fully responsible for it [30,31]. Lower circulatory insulin levels upon galactose consumption as we previously reported [13] result in lower glucose uptake and lower glycolysis levels, while lipolysis becomes less inhibited and provides more fatty acids for FAO. A major role for insulin may also explain why we did not observed difference in FAO gene expression the liver, the main galactose metabolic organ. If a differential insulin response is the main contributing factor at the whole body level, it would be of interest to study skeletal muscle and adipose tissue as the main insulin sensitive tissues.

In contrast to the whole-body increase in both relative (lower RER) and absolute lipid oxidation (Fig. 2C, F, and G), fatty acid oxidation (FAO) in the small intestinal mucosa of galactose-fed mice was reduced. This reduction in FAO may serve to spare fatty acids for oxidation elsewhere in the body, potentially explaining the absence of effects on whole-body energy expenditure (EE), body weight (BW), and body composition. The decrease in FAO was accompanied by lower expression of lipid droplet-associated transcripts (Fig. 5A and B) and a corresponding reduction in lipid droplets themselves (Fig. 5C). This aligns with the idea that the small intestine plays a role in supporting whole-body lipid oxidation, despite no observed increase in chylomicron-associated gene expression. Furthermore, an increase in intestinal fatty acid (FA) efflux is not supported by the lack of difference in serum triglyceride (TG) levels. However, this may be explained by increased FA utilization at whole body level, although, again in liver we did not observe differences in TG levels. Overall, dietary galactose strongly influences lipid metabolism in the small intestine, reducing both FAO and FA storage. These findings highlight an intestine-specific response that may contribute to whole-body energy homeostasis.

In our previous work, where mice were sacrificed in a food deprived state, we showed more profound differential effects in carbohydrate metabolism, concomitant with a lack of regulation of fatty acid metabolism in the small intestinal mucosa [9]. This is fully in line with the now observed lower expression of FAO transcripts in mice sacrificed in the fed state. In a food deprived state, enterocytes would rely more on FAO, making those pathways the main source of cellular energy. On the other hand, in a fed state, with a constant supply of nutrients mainly from the apical side, intestinal cells can rely more on carbohydrate oxidation as a source. In our previous and current data we observe that in the small intestine galactose has a profound effect on the “secondary pathway” of each metabolic state (carbohydrate oxidation during the food deprived state, and FAO during the fed state). Altogether, this suggests a facilitating role for the small intestine. In the here studied fed state, galactose induced an increased small intestinal reliance on carbohydrates as main energy source, allowing other organs to show the opposite, an increased FA utilization.

In addition to effects on FAO pathways, lipid synthesis pathways in small intestinal mucosa showed little differences, despite almost all PPP enzymes showing a lower expression in the galactose group. The PPP provides NADPH for lipid synthesis, but also for redox homeostasis. While lipid synthesis is only mildly affected, redox homeostasis is. The decreased PPP is thus in line with the decreased expression of NADP-dependent antioxidant enzymes, supported by the high correlations of transcript levels of FAO and NADPH generating enzymes (Supplemental Table 3). In addition, also the gene expression of NADPH-independent antioxidant enzymes *Sod1* and *Cat* are decreased, strongly suggesting a lower level of intestinal mucosal oxidative stress in the galactose group. We speculate that this is very likely attributable to a lower level in these cells of FAO, a known source of ROS [32].

In summary, our study demonstrates that the main effect of galactose consumption during the post-weaning period of fed female mice mainly lowers FAO and storage in the proximal small intestine, and thereby facilitates an increase in relative and absolute lipid utilization at the whole-body level. Decreases in gene expression of antioxidant and NADPH producing enzymes are in line with the decreased FAO, a known source of ROS. The upregulation of *Ppargc1a* suggests an increase in intestinal energy efficiency, possibly via the known galactose effects on mitochondrial OXPHOS. These findings provide valuable insights into the *in vivo* metabolic adaptations induced by dietary galactose and shed a new light on the organ specific metabolic roles.

Declaration of competing interests

The authors declare that they have no known competing financial interests or personal relationships that could have appeared to influence the work reported in this paper.

CRediT authorship contribution statement

Ferran S. Fos-Codoner: Writing – review & editing, Writing – original draft, Visualization, Validation, Methodology, Investigation, Funding acquisition, Formal analysis, Conceptualization. **Jaap Keijer:** Writing – review & editing, Writing – original draft, Visualization, Project administration, Funding acquisition, Conceptualization. **Melissa Bekkenkamp-Grovenstein:** Writing – review & editing, Methodology, Investigation. **Evert M. van Schothorst:** Writing – review & editing, Writing – original draft, Visualization, Validation, Project administration, Investigation, Funding acquisition, Formal analysis, Data curation, Conceptualization.

Acknowledgments

The authors would like to thank the staff of the Wageningen University animal facility CARUS for their assistance in the execution of the animal experiment, and Marina Kostopoulou for her experimental contribution and Margaret Bosveld for her help in HPAEC analysis. This project was funded by TKI–TopSector Agri & Food, Project number LWV20.387.

Supplementary materials

Supplementary material associated with this article can be found, in the online version, at doi:10.1016/j.jnutbio.2025.110193.

References

[1] Pearce J, Taylor MA, Langley-Evans SC. Timing of the introduction of complementary feeding and risk of childhood obesity: a systematic review. Int J Obes (London) 2013;37:1295–306.
[2] Shaoul R, Tiosano D, Hochberg Z. Evo-devo of child growth: the role of weaning in the transition from infancy to childhood. Crit Rev Food Sci Nutr 2016;56:887–95.
[3] Schaafsma G. Lactose and lactose derivatives as bioactive ingredients in human nutrition. Int Dairy J 2008;18:458–65.
[4] Stephen A, Alles M, de Graaf C, Fleith M, Hadjilucas E, Isaacs E, et al. The role and requirements of digestible dietary carbohydrates in infants and toddlers. Eur J Clin Nutr 2012;66:765–79.
[5] Rossignol R, Gilkerson R, Aggeler R, Yamagata K, Remington SJ, Capaldi RA. Energy substrate modulates mitochondrial structure and oxidative capacity in cancer cells. Cancer Res 2004;64:985–93.
[6] Holden HM, Rayment I, Thoden JB. Structure and function of enzymes of the leloir pathway for galactose metabolism. J Biol Chem 2003;278:43885–8.
[7] Conte F, van Buuringen N, Voermans NC, Lefeber DJ. Galactose in human metabolism, glycosylation and congenital metabolic diseases: time for a closer look. Biochim Biophys Acta Gen Subj 2021:1865.
[8] JanssenDuijghuijsen LM, Grefte S, de Boer VCJ, Zeper L, van Dartel DAM, van der Stelt I, et al. Mitochondrial ATP depletion disrupts caco-2 monolayer integrity and internalizes claudin 7. Front Physiol 2017;1–13(8):129898 8.
[9] Fos-Codoner FS, Bouwman LMS, Keijer J, van Schothorst EM. Dietary galactose increases the expression of mitochondrial OXPHOS genes and modulates the carbohydrate oxidation pathways in mouse intestinal mucosa. J Nutr 2023;153:3448–57.
[10] Fernández-Calleja JMS, Bouwman LMS, Swarts HJM, Oosting A, Keijer J, Van Schothorst EM. Direct and long-term metabolic consequences of lowly vs. highly-digestible starch in the early post-weaning diet of mice. Nutrients 2018;10(11):1788.
[11] Hoevenaars FPM, Van Schothorst EM, Horakova O, Voigt A, Rossmeisl M, Pico C, et al. BIOCLAIMS standard diet (BIOsd): a reference diet for nutritional physiology. Genes Nutr 2012;7:399–404.
[12] Bouwman LMS, Fernández-Calleja JMS, van der Stelt I, Oosting A, Keijer J, van Schothorst EM. Replacing part of glucose with galactose in the postweaning diet protects female but not male mice from high-fat diet–Induced adiposity in later life. J Nutr 2019;149(7):1140–8.
[13] Bouwman LMS, Swarts HJM, Fernández-Calleja JMS, van der Stelt I, Schols H, Oosting A, et al. Partial replacement of glucose by galactose in the post-weaning diet improves parameters of hepatic health. J Nutr Biochem 2019;73:108223.
[14] Fernández-Calleja JMS, Bouwman LMS, Swarts HJM, Oosting A, Keijer J, van Schothorst EM. Extended indirect calorimetry with isotopic CO2 sensors for prolonged and continuous quantification of exogenous vs. total substrate oxidation in mice. Sci Rep 2019;9:11507.
[15] Müller TD, Klingenspor M, Tschöp MH. Revisiting energy expenditure: how to correct mouse metabolic rate for body mass. Nat Metab 2021;3:1134–6.
[16] Gan Z, Klein CJMI, Keijer J, van Schothorst EM. Quantitative interpretation and modeling of continuous nonprotein respiratory quotients. Am J Physiol Endocrinol Metab 2025;328:E289–96.
[17] Péronnet F, Massicotte D. Table of nonprotein respiratory quotient: an update. Can J Sport Sci 1991;16:23–9.
[18] Andrews S. FastQC: Quality control tool for high throughput sequence data 2010. Accessed date: 21 March 2024, Available online at: http://www.bioinformatics.babraham.ac.uk/projects/fastqc/.
[19] Dobin A, Davis CA, Schlesinger F, Drenkow J, Zaleski C, Jha S, et al. STAR: ultrafast universal RNA-seq aligner. Bioinformatics 2013;29(1):15–21.
[20] Anders S, Pyl PT, Huber W. HTSeq—A Python framework to work with high-throughput sequencing data. Bioinformatics 2015;31(2):166–9.
[21] Love MI, Huber W, Anders S. Moderated estimation of fold change and dispersion for RNA-seq data with DESeq2. Genome Biol 2014;15(12):550.
[22] Yu G, Wang LG, Han Y, He QY. ClusterProfiler: an R package for comparing biological themes among gene clusters. Omi A J Integr Biol 2012;16:284–7.
[23] Puigserver P, Spiegelman BM. Peroxisome proliferator-activated receptor-gamma coactivator 1 alpha (PGC-1 alpha): transcriptional coactivator and metabolic regulator. Endocr Rev 2003;24:78–90.
[24] Kersten S, Stienstra R. The role and regulation of the peroxisome proliferator activated receptor alpha in human liver. Biochimie 2017;136:75–84.
[25] Kersten S. Integrated physiology and systems biology of PPARα. Mol Metab 2014;3:354–71.
[26] D'Aquila T, Sirohi D, Grabowski JM, Hedrick VE, Paul LN, Greenberg AS, et al. Characterization of the proteome of cytoplasmic lipid droplets in mouse enterocytes after a dietary fat challenge. PLoS One 2015;10(5):e0126823.
[27] Dominiczak MH, Caslake MJ. Apolipoproteins: metabolic role and clinical biochemistry applications. Ann Clin Biochem 2011;48:498–515.
[28] Cuatrecasas P, Segal S. Mammalian galactose dehydrogenase. J Biol Chem 1966;241:5904–9.
[29] Mohammad MA, Sunehag AL, Rodriguez LA, Haymond MW. Galactose promotes fat mobilization in obese lactating and nonlactating women. Am J Clin Nutr 2011;93(2):374–81.
[30] Stahel P, Kim JJ, Xiao C, Cant JP. Of the milk sugars, galactose, but not prebiotic galacto-oligosaccharide, improves insulin sensitivity in male Sprague-Dawley rats. PLoS One 2017;12(2):e0172260.
[31] Ercan N, Nuttall FQ, Gannon MC, Redmon JB, Sheridan KJ. Effects of glucose, galactose, and lactose ingestion on the plasma glucose and insulin response in persons with non-insulin-dependent diabetes mellitus. Metabolism 1993;42:1560–7.
[32] Morant-Ferrando B, Jimenez-Blasco D, Alonso-Batan P, Agulla J, Lapresa R, Garcia-Rodriguez D, et al. Fatty acid oxidation organizes mitochondrial supercomplexes to sustain astrocytic ROS and cognition. Nat Metab 2023;5:1290–302.